Medical Engineering and Physics 73 (2019) 100–106

Contents lists available at ScienceDirect

Medical Engineering and Physics

journal homepage: www.elsevier.com/locate/medengphy

Technical note

Design of an isokinetic knee dynamometer for evaluation of functional electrical stimulation strategies

Efe Anil Aksöz[a,b], Marco Laubacher[a,b], Robert Riener[b], Kenneth J. Hunt[a,*]

[a] Institute for Rehabilitation and Performance Technology, Division of Mechanical Engineering, Department of Engineering and Information Technology, Bern University of Applied Sciences, Burgdorf CH-3400, Switzerland
[b] Sensory Motor Systems Lab, Institute of Robotics and Intelligent Systems, Department of Health Sciences and Technology, ETH Zürich, CH-8000 Zürich, Switzerland

ARTICLE INFO

Article history:
Received 9 October 2018
Revised 9 July 2019
Accepted 18 July 2019

Keywords:
Functional electrical stimulation
FES cycling
Control systems
Knee joint torque
Knee extension
Rehabilitation robots

ABSTRACT

Background: The limitations of functional electrical stimulation (FES) cycling directly affect the health benefits acquired from this technology and prevents its' full potential to be realised. Experiments should be done on a test bed which can isolate and focus only on one muscle group, namely the quadriceps. The aim of this work was to design and develop an isokinetic robotic leg extension/flexion dynamometer which can mimic knee joint motion during actual cycling to be used for evaluation of novel functional electrical stimulation strategies. Although the main motivation for development of the dynamometer was for application in FES studies, it has the potential to be used for various different muscle physiology studies.

Methods: A feedback control system with integrated electrical stimulation for isokinetic knee joint torque measurement has been developed and tested for safety and functionality. The leg extension/flexion device was modified and equipped with a DC motor drive system to imitate isokinetic knee joint motion during cycling when the hip joint remains fixed. Real-time bi-directional effective torque on the lever arm was measured by a magnetostrictive torque sensor and a load cell. Closed-loop motor control system was also designed to mimic the cyclical motion at desired angular velocity.

Results: A functional model of the robotic dynamometer was developed and evaluated. The dynamometer is capable of simulating the knee angle during cycling at a cadence of up to 70 rpm with range of motion of 72°. The magnetostrictive torque sensor can measure torque values up to 75 Nm. The lever arm can be adjusted and the target knee angle was controlled with RMSE tracking error of less than 2.1° in tests with and without a test person, and with and without muscle stimulation.

Conclusions: The isokinetic knee joint torque measurement system was designed and validated in this work, and subsequently used to develop and evaluate novel muscle activation strategies. This is important for fundamental research on effective stimulation patterns and novel activation strategies. This will, in turn, enhance the efficiency of FES cycling exercise and has the potential to improve the health-beneficial effects.

1. Introduction

Functional electrical stimulation (FES) is a technique to evoke contractions in paralysed muscles by applying electrical impulses to motor nerves [1] and it is used as part of the rehabilitation programme for individuals with spinal cord injury (SCI) for functional improvements such as muscle strength [2,3]. FES cycling, one of the applications of this technology, achieved by functional electrical stimulation of paralysed leg muscles promotes various physiological and functional improvements in paralysed limbs [4–6].

Notation and Abbreviations: θ, Knee angle; θ^*, Desired knee angle; e, Error $(\theta^* - \theta)$; $C(s)$, Linear Compensator; ω^*, Desired angular velocity; ω_m, Measured angular velocity; e_m, Error $(\omega^* - \omega_m)$; C_m, Linear Compensator, motor control; u_m, Control signal, motor control; M, Motor; d, Disturbance; $P_o(s)$, Nominal plant; $A_o(s)$, Polynomial (plant denominator); $B_o(s)$, Polynomial (plant numerator); k, Steady-state gain; τ, Time constant; $\Phi(s)$, Characteristic polynomial; ω_n, Natural frequency; T_s, Sample period; τ_s, Measured torque sensor value; τ_l, Measured load-cell value; τ_m, Measured motor torque; F_l, Leg force; F_c, Chain force; P_m, Measured overall power.

* Corresponding author.
E-mail address: kenneth.hunt@bfh.ch (K.J. Hunt).

https://doi.org/10.1016/j.medengphy.2019.07.010

Since lower-limb FES cycling elicits a low cardiovascular response, there are two possible ways forward: the first is to use knowledge gained from the new device to optimise and enhance the aerobic response from lower-limb cycling (this is the focus of the present work); the second is to introduce the arms to give hybrid leg-arm exercise. FES leg cycling is often combined with voluntary arm cranking [7,8] which gives higher oxygen uptake than leg cycling only. Lower-limb FES cycling has been shown to improve cardiovascular and respiratory function [9–11] body composition, muscle mass [12], bone mass [13] and life quality after spinal cord injury [14–18].

Although FES cycling has a variety of health benefits and brings substantial advantagefor people with SCI, various studies highlighted its current limitations [19–24] and showed that the full potential of this technology has not yet been achieved. In order to address these limitations, new activation patterns were investigated when the subjects were in a fixed seating position and performing isometric exercise; thus, there is a need for isokinetic measurements using a dynamometer, which better matches dynamic cycling exercise.

Existing commercial dynamometer systems generally do not integrate FES, and are not specifically designed to mimic knee-joint dynamics typical of recumbent cycling. Available devices include System 4 Pro (Biodex Medical Systems Inc., USA), Humac Norm (Computer Sports Medicine Inc., USA) [25], Genu PLUS (Easytech LLC, Italy), S2P dynamometer (S2P, Science to Practice Ltd., Slovenia) and the Motionmaker (Swortec SA, Switzerland). Apart from the Motionmaker, these dynamometers are not equipped with FES stimulators, but Motionmaker is not able to mimic cycling motion at a typical cycling cadence. Although the mentioned commercial devices can be modified with an FES stimulator to be used for experiments, a custom made isokinetic knee dynamometer equipped with FES stimulation and sensor technology is needed for cost-effective solution (the cost of the device presented here was approximately CHF 3000).

The aim of this work was to design and develop an isokinetic robotic leg extension/flexion dynamometer which can mimic knee joint motion during actual cycling to be used for evaluation of novel functional electrical stimulation strategies. Although the main motivation for development of the dynamometer was for application in FES studies, it has the potential to be used for various different muscle physiology studies. For example, it could be used to investigate the relationship between muscle size and strength [26], age-related effects [27] or changes in muscle strength after weight reduction [28], leg dominance effects [29] and also for cortical bone studies [30].

2. Methods

A novel isokinetic knee joint torque measurement system (knee dynamometer) was designed and constructed. Mechanical, electrical, feedback control and electrical stimulation systems for the isokinetic knee joint torque measurement system were developed and the system was tested for safety and functionality.

2.1. Equipment

A seated leg extension/curl bench (RLE-382, Tuffstuff Fitness International Inc., USA) was used as the base frame of the dynamometer to ensure safety, comfort and durability. The base was then modified and equipped with an actuator system to move the legs by imitating isokinetic knee joint motion during cycling when the hip joint remains fixed, and with an FES system (Fig. 1).

The actuator system is composed of a brushless motor (EC45, 250 W, Maxon AG, Switzerland) and a planetary gear-head (GP52C, Maxon AG, Switzerland) with a gear ratio of 156:1. The actuator system is connected to the lever arm via a chain drive system. The lever arm is placed in the middle of the seat (i.e., between the test person's legs) to be able to attach and move each leg separately and independently. To obtain a target knee-joint angle (knee extension angle, 180° when fully extended) trajectory which mimics actual cycling, the range of motion of the lever arm was obtained from the recumbent tricycle by using a basic goniometer and 2D marker based tracking of knee joint during cycling (Fig. 2). The seating position of the ergometer can be manually adjusted in order to match the seating position in recumbent cycling.

The actuator system can generate a maximum continuous torque of 48.52 Nm. This value is then increased to a maximum torque value of 80 Nm with gear ratio of the sprockets (40:24) in the chain drive system. Typical cadence values in FES-cycling are

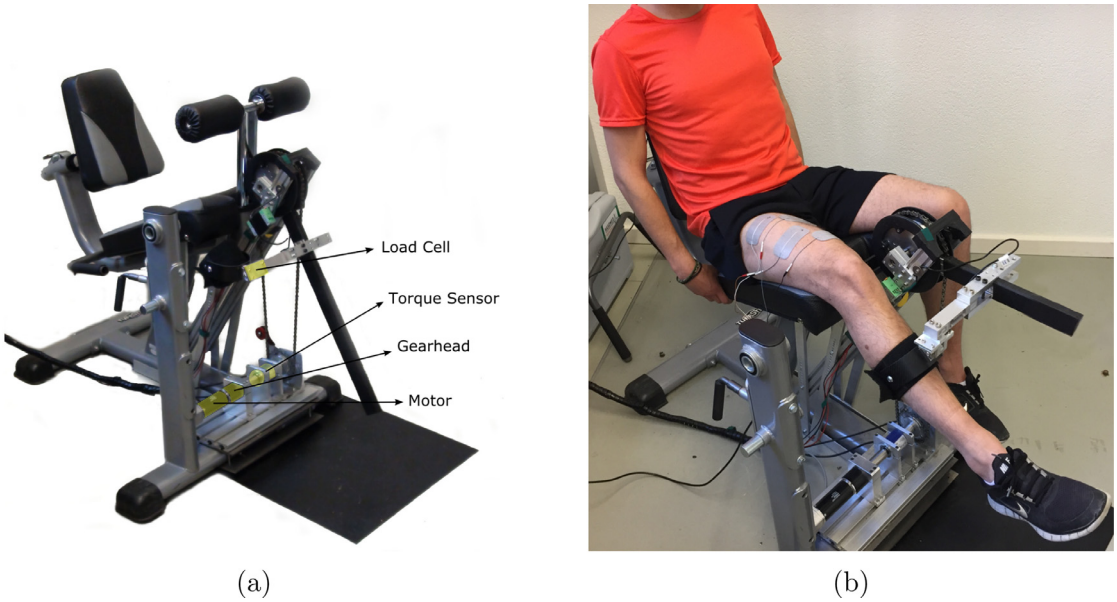

Fig. 1. Isokinetic knee joint torque measurement system (knee dynamometer). (a) Device and components. (b) Device with test person with surface electrodes on the right quadriceps.

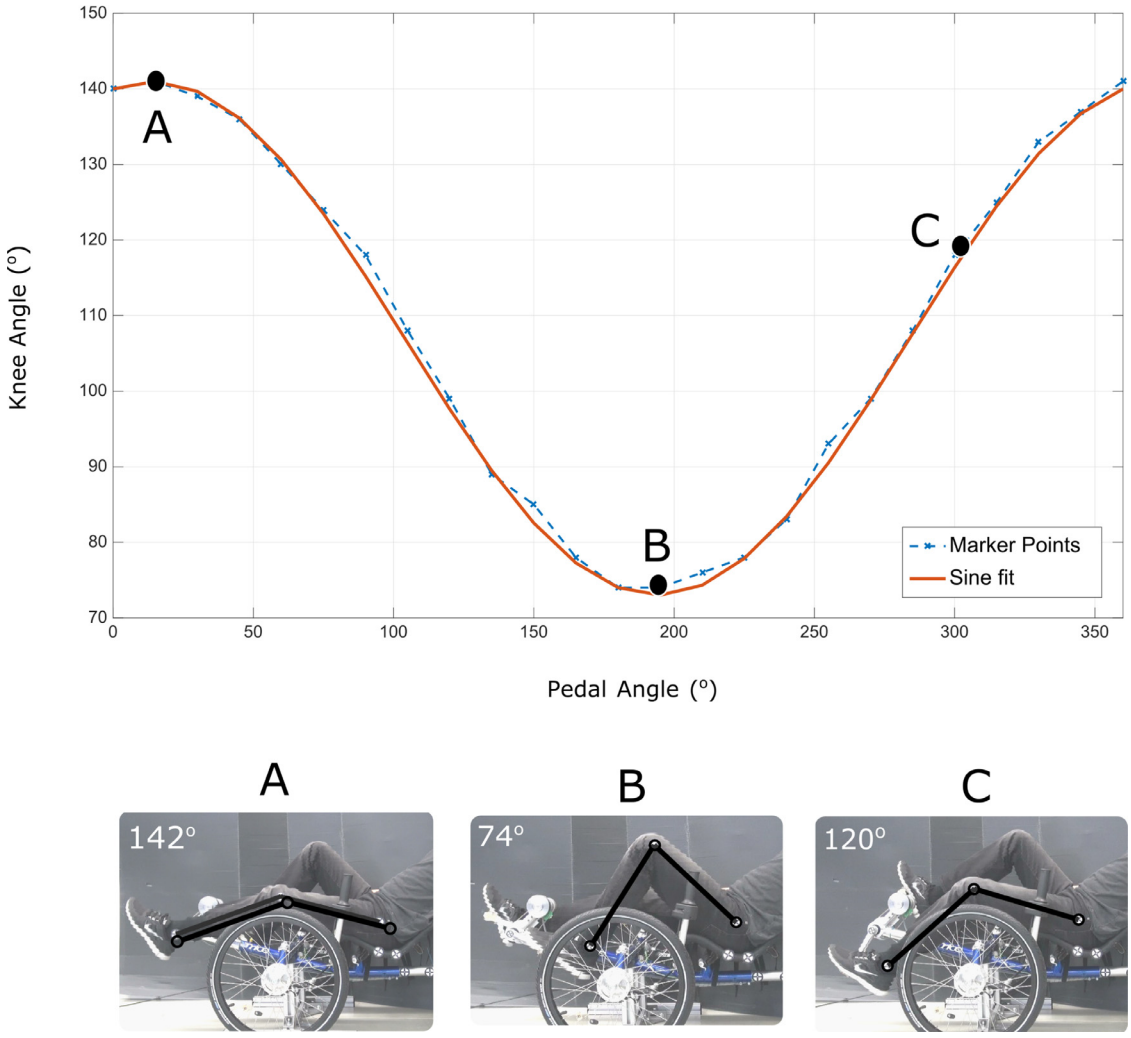

Fig. 2. 2D Marker-based tracking graph for knee angle detection during cycling. 3 different knee position (A, B, C) on the trike (142°, 74° and 120°) are marked on the graph.

up to 50 rpm, and the knee dynamometer was designed to control to an arbitrary cadence value above and below this range.

2.2. Sensors

A magnetostrictive torque sensor (Series 2000, NCTE AG, Germany) is placed in between the actuator system and the chain drive system to reduce the mechanical friction disturbance in torque measurement. By that, the actuator system can apply the needed torque (for resistance or support) without any interaction with the sensor. The torque sensor is used to measure the effective torque applied on the pivot arm in real time during both isokinetic motion and rest phase. The torque value was cross calibrated with a load cell (LCB130, Transmetra, Switzerland) and motor current values. An analogue position sensor (Vert-X, Contelec AG, Germany) is used for angle measurement with a resolution of 0.648°. For critical measurements, the resolution can improved to 0.004° by using hall sensors in the actuator. The magnetostrictive torque sensor can measure torque values up to 75 Nm at 1000 Hz with an accuracy of 1 % and 0.05 % repeatability (manufacture's data).

2.3. Feedback control model

A software program was developed for isokinetic torque measurements and for real time feedback control of the target knee-angle trajectory. The user interface was implemented with a Matlab graphical user interface (GUI) module and the movement is controlled with a Matlab/Simulink model (Mathworks Inc., USA). Closed-loop control strategy is implemented to generate the desired isokinetic motion. Analog and digital filters are used for accurate, noise free measurements.

Real-time acquisition of input and output signals, as well as statistical analysis of the data are carried out by the custom-made software program. All raw and filtered parameters are stored for future use. The control model diagram can be seen in Figures 3 and 4.

The nominal plant that is used for mathematical derivation and calculation of the controller is denoted $P_o(s)$. This transfer function links the target angular velocity and measured position (angle) of the lever arm. This relationship is simply an integrator, thus

$$\omega^* \rightarrow \theta : P_o(s) = \frac{B_o(s)}{A_o(s)} = \frac{k}{s}. \quad (1)$$

Here, the polynomials $A_o(s)$ and $B_o(s)$ are defined as $A_o(s) = s$ and $B_o(s) = k$, the latter representing the integrator gain. In order to exactly compute the parameters of the linear, time-invariant compensator $C(s)$, a pole-assignment design approach was followed. The compensator transfer function $C(s)$ was constrained to be strictly proper in order to achieve gain rolloff as frequency increases. $C(s)$ thus had the form

$$C(s) = \frac{G(s)}{H(s)} = \frac{g_0}{(s + h_0)} \quad (2)$$

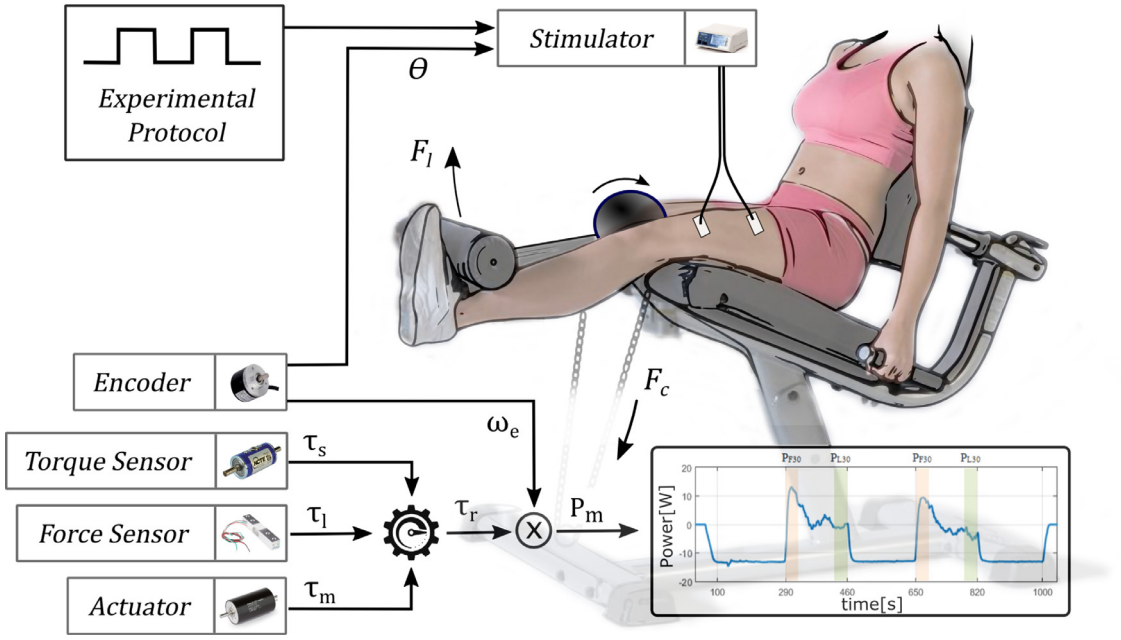

Fig. 3. Knee dynamometer control diagram. Measured values (sensor torque, τ_s, load-cell torque, τ_l, motor torque, τ_m), calibrated real torque value (τ_r), angular velocity (ω_e), knee angle (θ), measured power (P_m), force values (chain force, F_c, leg force, F_l).

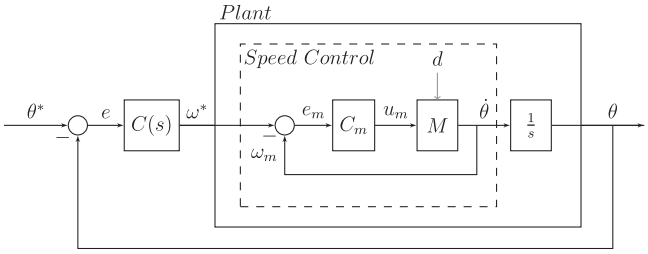

Fig. 4. Knee dynamometer control block diagram. Speed control, which is implemented in the motor controller, is in the dashed box. The effective controlled plant includes the speed control block and an integrator.

where the real coefficients g_0 and h_0 are to be determined following the pole assignment approach. It is readily observed that the polynomials $G(s)$ and $H(s)$ are $G(s) = g_0$ and $H(s) = (s + h_0)$. Because the plant naturally includes an integrator, the compensator does not require to contain integral action. The characteristic polynomial of the feedback system of Figure 4, $\Phi(s)$, is

$$\Phi(s) = s(s + h_0) + kg_0. \tag{3}$$

Thus, since the degree of Φ is 2, the general form of Φ is

$$\Phi(s) = s^2 + \phi_1\, s + \phi_0 \tag{4}$$

and the coefficients ϕ_0 and ϕ_1 are determined by arbitrary placement of the two closed-loop poles in the s-plane. Here, Φ was set according to the damping ratio ζ and natural frequency ω_n, giving

$$\Phi(s) = s^2 + 2\zeta\omega_n s + {\omega_n}^2. \tag{5}$$

The unknown controller parameters g_0 and h_0 are then determined by matching coefficients of equal powers in s in Eqns. (3) and (5),

$$h_0 = 2\zeta\omega_n,\ \ g_0 = \omega_n^2/k. \tag{6}$$

When ζ is close to 1, natural frequency ω_n is related to rise time as $\omega_n = 3.35/tr$. In the following, critical damping with $\zeta = 1$ is employed. The rise time was set to $t_r = 0.2$ and the plant gain is $k = 1$. From Eqs. (2) and (6), the compensator is

$$C(s) = \frac{{\omega_n}^2/k}{s + 2\zeta\omega_n} \tag{7}$$

The accuracy of feedback control of the target knee-joint angle was quantified using RMS tracking error,

$$\mathrm{RMSE} = \sqrt{\sum_{t=t_0}^{t_1} (\theta_{nom}(t) - \theta(t))^2} \tag{8}$$

where $\theta_{nom}(t)$ is the simulated position, obtained using the nominal model and the calculated feedback controller, and $\theta(t)$ is the actual measured position value. t_0 and t_1 are the start and end times of the RMS tracking error evaluation period.

2.4. Stimulation

An 8-channel stimulator (Rehastim, Hasomed GmbH, Germany) was integrated and synchronised with the dynamometer system. The stimulation parameters that can be adjusted in real time using Rehastim science mode are: amplitude (0–127 mA), pulse width (0–500 µs), number of channels (1–8), frequency (0–100 Hz) and stimulation mode (singlet, doublet, triplet). Parameters can be directly set manually by using the graphical user interface or automatically within the Simulink control model in real time. In order to avoid problems caused by instantaneous changes in stimulation parameters, all parameters can be gradually changed (ramped up/down) over time. The ramp time can be set manually before each experiment and/or in real time.

To illustrate a typical power-output analysis during tests to evaluate new stimulation strategies, mechanical power output was assessed with a short-term test where the test person was stimulated using 2 channels and surface electrodes attached to motor points on the right quadriceps. Motor points were found with a motor point pen during a familiarisation phase.

Different stimulation patterns such as stochastically-modulated inter-pulse intervals (IPI), spatially distributed sequential stimulation (SDSS) electrodes and variable amplitude and pulse-width trains can be set for each stimulation phase. Stimulation was active only during the leg extension phase of the exercise, where

the angular velocity is positive and the angle of the lever arm is within the stimulation angle range. This can be adjusted arbitrarily depending on the range of motion of the lever arm. Usually, during cycling motion, the quadriceps are stimulated slightly later than the start of the knee extension phase. The default stimulation range is thus set with a 10° offset.

2.5. Measurement protocol

To illustrate a typical power-output analysis during tests to evaluate new stimulation strategies, mechanical power output was assessed with a short-term test where the test person was stimulated using 2 channels and surface electrodes attached to motor points on the right quadriceps. Motor points were found with a motor point pen during a familiarisation phase. Stimulation parameters including pulse width, amplitude, and frequency as well as angular velocity, torque and angle of the lever arm are saved with a sample time of 0.01 s. The date of the experiment and details on the test person are collected from the graphical user interface of the simulink model. All raw and filtered sensor data are saved separately for further evaluation.

To demonstrate the function and performance of the system, a series of experiments with an able-bodied test person are reported here. The feedback control system was tested and, in dynamic tests with three different conditions, RMSE tracking error was calculated.

3. Results

Under test condition A, the lever arm was moved without the test person and followed the target angle with RMSE tracking error of 1.7°. During the tests with the test person who remained passive, the position control system had RMSE tracking error of 1.9° without stimulation (condition B), and lastly test condition C, where stimulation was used (stimulation parameters: 100 µs, 40 mA, 35 Hz), the feedback control system followed the desired position with RMSE tracking error of 2.1° (Fig. 5). The range of motion of the lever arm was found to be 74°–142° from the manual goniometer measurement and position tracking.

Power output was measured during assisted knee extension: Figure 6 shows the average power curve from the measurement (Stimulation parameters: 100 µs, 40 mA, 35 Hz, time: 6 min). The mean power (P_{mean} = 22 W) and the peak power (P_{peak} = 47 W) can be measured for each extension or as an average.

4. Discussion

The aim of this work was to design and develop an isokinetic robotic leg extension/flexion dynamometer which can mimic knee joint motion during actual cycling to be used for evaluation of novel functional electrical stimulation strategies.

The range of motion of the knee joint (72°) during cycling was precisely measured during recumbent cycling and successfully transferred to the dynamometer. Position controller design was

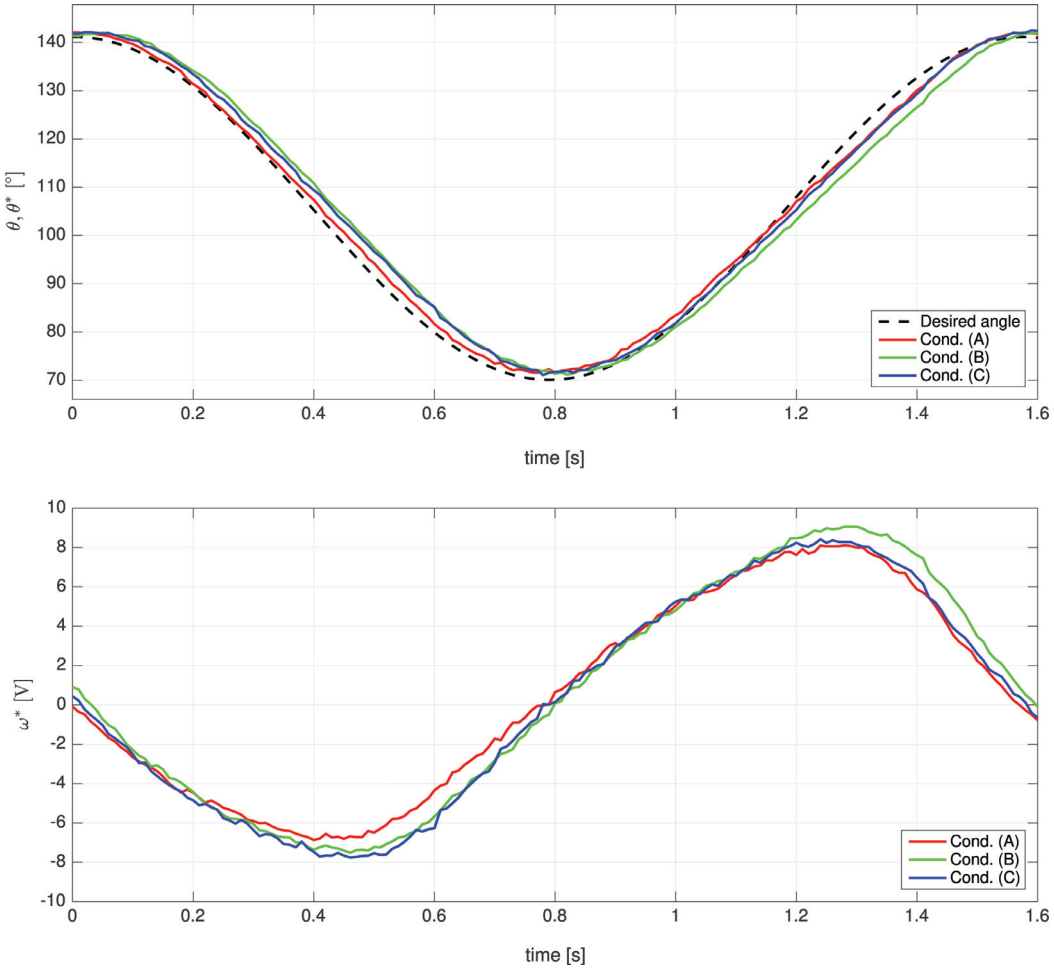

Fig. 5. Dynamic test with angular velocity controller. Condition (A) shows the results of the experiment with no test person on the device, condition (B) with a test person and no stimulation and condition (C) with a test person and stimulation.

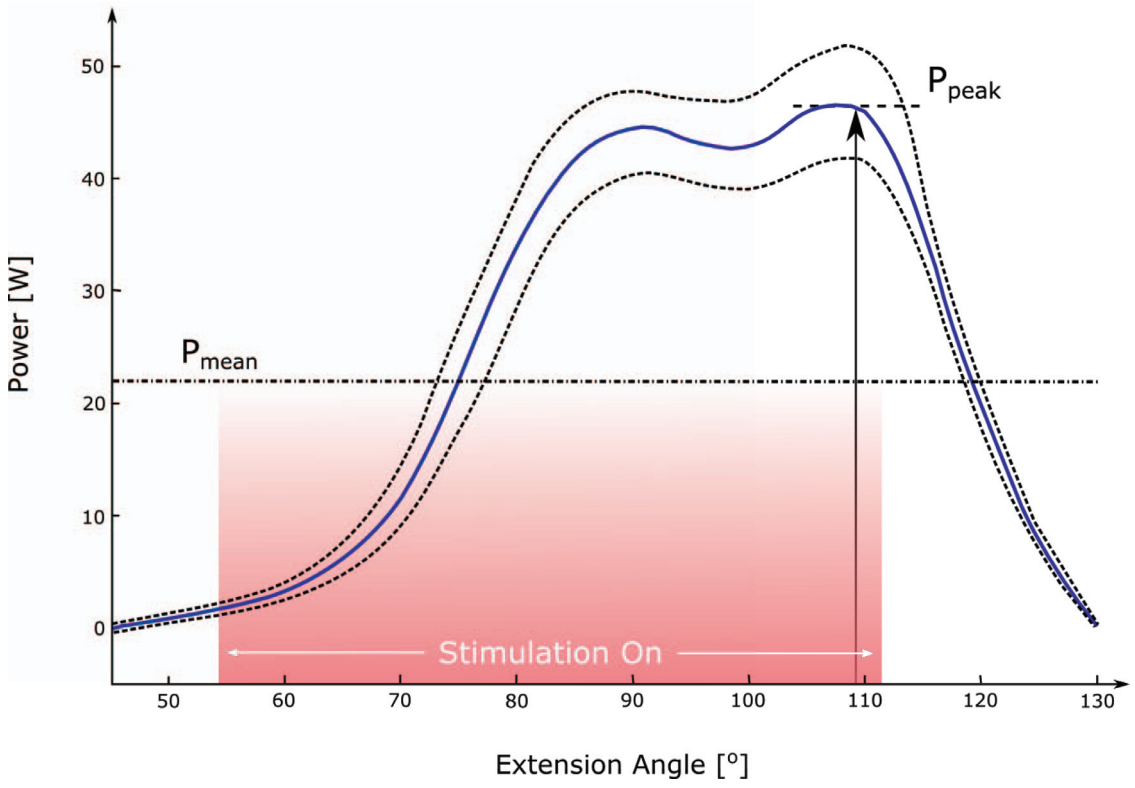

Fig. 6. Power curve during knee extension with 6 min of stimulation of one leg. Mean power (P_{mean}) and peak power output (P_{peak}) are marked with dash-dot line and dashed line, respectively. Stimulation pulse-width was 100 μs and the amplitude was 40 mA during the experiment. Blue solid line shows the mean power curve, dashed lines are bounds showing the minimum and maximum measurements. The shaded area shows the angle range when the stimulation was on.

based on a simple plant model to mimic the cycling motion accurately and the device functionality was dynamically tested with and without a test person on the device, and with/without stimulation. The feedback control performance was tested across the range of different conditions and it was proved to be accurate and robust. RMSE tracking error of the feedback control system was calculated and demonstrated precise position control of less than around 2° under all conditions tested.

The safety of the device was assured by using mechanical brakes, emergency stop buttons and excessive torque monitoring and prevention systems. Actuator and chain drive systems were designed as back-drivable, which is crucial when the motors shut down because of any possible error. By using position and angular velocity measurements, electrical stimulation is enabled only in the desired range of stimulation angle. When a problem occurs because of the surface electrodes, the stimulator's internal safety system activates to stop stimulation in order to prevent electrical pulses to reach the muscle groups. Also, the graphical user interface of the control model was designed to give error feedback before and during the tests to inform the user.

The dynamometer had been used as a test-bed in various separate studies to assess new activation patterns and novel electrode configurations to optimise the efficiency of FES cycling. The effect of stochastic modulation of inter-pulse intervals was investigated with experiments carried out on the knee dynamometer [31]. Seven able-bodied test persons were tested on the device and mechanical power output was compared during 3 min stimulation with constant and 3 min randomised IPI. Statistically significantly higher power output values were observed during randomised IPI stimulation. Spatially distributed sequential stimulation was also tested in a dynamic knee-extension task and significantly higher power output and reduced fatigue were observed [32]. Lastly, proximally and distally placed spatially distributed sequential stimulation electrodes were compared by using the knee dynamometer [33] and outcomes suggested no significant difference between those two different strategies.

5. Conclusions

An isokinetic knee joint torque measurement system was designed and validated in this work, and subsequently used to develop and evaluate novel muscle activation strategies. This is important for fundamental research on effective stimulation patterns and novel activation strategies. This will, in turn, make FES cycling a more efficient rehabilitation technique and has the potential to improve the health-beneficial effects.

Ethics approval and consent to participate

The research described in this article was performed in accordance with the Declaration of Helsinki. Measurement protocols were reviewed and approved by the Ethics Committee of the Swiss Canton of Bern. All participants provided written, informed consent.

Funding

This work was supported by the Swiss National Science Foundation (SNSF grant number: 320030_150128).

Declaration of Competing Interest

We wish to confirm that there are no known conflicts of interest associated with this publication and there has been no significant financial support for this work that could have influenced its outcome.

CRediT authorship contribution statement

Efe Anil Aksöz: Conceptualization, Data curation, Formal analysis, Methodology, Project administration, Software, Writing - review & editing, Writing - original draft. **Marco Laubacher:** Methodology, Validation, Writing - review & editing. **Robert Riener:** Supervision, Writing - review & editing. **Kenneth J. Hunt:** Conceptualization, Investigation, Project administration, Resources, Supervision, Writing - review & editing.

References

[1] Stein RB, Chong SL, James KB, Kido A, Bell GJ, Tubman LA, et al. Electrical stimulation for therapy and mobility after spinal cord injury. Prog Brain Res 2002;137:27–34.

[2] Maffiuletti NA. Physiological and methodological considerations for the use of neuromuscular electrical stimulation. Eur J Appl Physiol 2010;110(2):223–34. doi:10.1007/s00421-010-1502-y. http://www.ncbi.nlm.nih.gov/pubmed/20473619.

[3] Schuhfried O, Crevenna R, Fialka-Moser V, Paternostro-Sluga T. Non-invasive neuromuscular electrical stimulation in patients with central nervous system lesions: an educational review. J Rehabil Med 2012;44(2):99–105. doi:10.2340/16501977-0941.

[4] Peckham PH, Knutson JS. Functional electrical stimulation for neuromuscular applications. Annu Rev Biomed Eng 2005;7(1):327–60.

[5] Gater DR, Dolbow D, Tsui B, Gorgey AS. Functional electrical stimulation therapies after spinal cord injury. NeuroRehabilitation 2011;28(3):231–48. doi:10.3233/NRE-2011-0652.

[6] Sheffler LR, Chae J. Neuromuscular electrical stimulation in neurorehabilitation. Muscle Nerve 2007;35(5):562–90. doi:10.1002/mus.20758. http://www.ncbi.nlm.nih.gov/pubmed/17299744.

[7] Berkelmans R, Duysens J, van Kuppevelt D. Development of a tricycle for spinal cord injured. Assist Technol Res Ser 2010;26(Rehabilitation: Mobility, Exercise and Sports):329–31. doi:10.3233/978-1-60750-080-3-329.

[8] Berkelmans R. Fes cycling. J Autom Control 2008;18(2):73–6. doi:10.2298/jac0802073b.

[9] Davis GM, Hamzaid NA, Fornusek C. Cardiorespiratory, metabolic, and biomechanical responses during functional electrical stimulation leg exercise: health and fitness benefits. Artif Organs 2008;32(8):625–9.

[10] Glaser R. Functional neuromuscular stimulation. Int J Sports Med 1994;15(03):142–8. doi:10.1055/s-2007-1021036.

[11] Berry HR, Perret C, Saunders BA, Kakebeeke TH, Donaldson N, Allan DB, et al. Cardiorespiratory and power adaptations to stimulated cycle training in paraplegia. Med Sci Sports Exerc 2008;40(9):1573–80.

[12] Duffell L, Donaldson N, Perkins T, Rushton D, Hunt KJ, Kakebeeke TH, et al. Long term intensive electrically stimulated cycling by spinal cord injured people; the effect on muscle properties and their relation to power output. Muscle Nerve 2008;38(4):1304–11.

[13] Frotzler A, Coupaud S, Perret C, Kakebeeke TH, Hunt KJ, Donaldson N, et al. High-volume FES-cycling partially reverses bone loss in people with chronic spinal cord injury. Bone 2008;43(1):169–76.

[14] Perkins T, Donaldson N, Hatcher N, Swain I, Wood D. Control of leg-powered paraplegic cycling using stimulation of the lumbo-sacral anterior spinal nerve roots. IEEE Trans Neural Syst Rehabil Eng 2002;10(3):158–64.

[15] Dolbow DR, Gorgey AS, Ketchum JM, Gater DR. Home-based functional electrical stimulation cycling enhances quality of life in individuals with spinal cord injury. Top Spinal Cord Injury Rehabil 2013;19(4):324–9.

[16] Dolbow DR, Gorgey AS, Daniels JA, Adler RA, Moore JR, Gater DR. The effects of spinal cord injury and exercise on bone mass: a literature review. NeuroRehabilitation 2011;29(3):261–9. doi:10.3233/NRE-2011-0702. http://www.ncbi.nlm.nih.gov/pubmed/22142760.

[17] Sköld C, Lönn L, Harms-Ringdahl K, Hultling C, Levi R, Nash M, et al. Effects of functional electrical stimulation training for six months on body composition and spasticity in motor complete tetraplegic spinal cord-injured individuals. J Rehabil Med 2002;34(1):25–32. http://www.ncbi.nlm.nih.gov/pubmed/11900259.

[18] Dolbow DR, Gorgey AS, Gater DR, Moore JR. Body composition changes after 12 months of FES cycling: case report of a 60-year-old female with paraplegia. Spinal Cord 2014;52. doi:10.1038/sc.2014.40. http://www.ncbi.nlm.nih.gov/pubmed/24902644.

[19] Szecsi J, Straube A, Fornusek C. A biomechanical cause of low power production during FES cycling of subjects with SCI. J Neuroeng Rehabil 2014;11(1):123. doi:10.1186/1743-0003-11-123.

[20] Hunt KJ, Fang J, Saengsuwan J, Grob M, Laubacher M. On the efficiency of FES cycling: a framework and systematic review. Technol Health Care 2012;20(5):395–422. doi:10.3233/THC-2012-0689.

[21] Hunt KJ, Saunders BA, Perret C, Berry H, Allan DB, Donaldson N, et al. Energetics of paraplegic cycling: a new theoretical framework and efficiency characterisation for untrained subjects. Eur J Appl Physiol 2007;101(3):277–85.

[22] Ibitoye MO, Hamzaid NA, Hasnan N, Abdul Wahab AK, Davis GM. Strategies for rapid muscle fatigue reduction during FES exercise in individuals with spinal cord injury: A systematic review. Plos One 2016;11(2). doi:10.1371/journal.pone.0149024.

[23] Thrasher A, Graham GM, Popovic MR. Reducing muscle fatigue due to functional electrical stimulation using random modulation of stimulation parameters. Artif Organs 2005;29(6):453–8. doi:10.1111/j.1525-1594.2005.29076.x.

[24] Marsden CD, Meadows JC, Merton PA. "Muscular wisdom" that minimizes fatigue during prolonged effort in man: peak rates of motoneuron discharge and slowing of discharge during fatigue. Adv Neurol 1983;39:169–211. http://www.ncbi.nlm.nih.gov/pubmed/6229158.

[25] Valovich-McLeod TC, Shultz SJ, Gansneder BM, Perrin DH, Drouin JM. Reliability and validity of the biodex system 3 pro isokinetic dynamometer velocity, torque and position measurements. Eur J Appl Physiol 2004;91(1):22–9. doi:10.1007/s00421-003-0933-0.

[26] Reid SL, Pitcher CA, Williams SA, Licari MK, Valentine JP, Shipman PJ, et al. Does muscle size matter? The relationship between muscle size and strength in children with cerebral palsy. Disab Rehabil 2014;37(7):579–84. doi:10.3109/09638288.2014.935492.

[27] Charlier R, Knaeps S, Mertens E, Van Roie E, Delecluse C, Lefevre J, et al. Age-related decline in muscle mass and muscle function in flemish caucasians: a 10-year follow-up. Age (Dordrecht, Netherlands) 2016;38:36. doi:10.1007/s11357-016-9900-7.

[28] Kim B, Tsujimoto T, So R, Zhao X, Oh S, Tanaka K. Changes in muscle strength after diet-induced weight reduction in adult men with obesity: a prospective study. Diabetes Metab Syndr Obes: Targets Ther 2017;10:187–94. doi:10.2147/dmso.s132707.

[29] Abdelmohsen AM. Leg dominance effect on isokinetic muscle strength of hip joint. J Chiropract Med 2019;18(1):27–32. doi:10.1016/j.jcm.2018.03.009.

[30] Higgins S, Sokolowski CM, Vishwanathan M, Anderson JG, Schmidt MD, Lewis RD, et al. Predicting diaphyseal cortical bone status using measures of muscle force capacity. Med Sci Sports Exerc 2018;50(7):1433–41. doi:10.1249/mss.0000000000001581.

[31] Aksöz EA, Laubacher M, Binder-Macleod SA, Hunt KJ. Effect of stochastic modulation of inter-pulse interval during stimulated isokinetic leg extension. Eur J Transl Myol 2016;26(3):229–34.

[32] Laubacher M, Aksöz EA, Riener R, Binder-Macleod S, Hunt KJ. Power output and fatigue properties using spatially distributed sequential stimulation in a dynamic knee-extension task. Eur J Appl Physiol 2017;117(9):1787–98.

[33] Laubacher M, Aksöz EA, Binder-Macleod S, Hunt KJ. Comparison of proximally versus distally placed spatially distributed sequential stimulation electrodes in a dynamic knee extension task. Eur J Transl Myol 2016;26(2):110–15.